International Journal of Technology

http://ijtech.eng.ui.ac.id

Research Article

Design and Simulation of a Quadruped Robot for Ground Contact Forces on Various Surfaces

Zaineb Wared Matteb[1*], Sadeq Hussein Bakhy[1], Nabil Hassan Hadi[2]

[1]Mechanical Engineering Department, College of Engineering, University of Technology, Al-Sina'a Street, Baghdad 10066, Iraq

[2]Aeronautical Engineering Department, College of Engineering, University of Baghdad, Baghdad 10072, Iraq

[*]Corresponding author: eng.zaineb@uomustansiriyah.edu.iq; Tel.: +9647718602336

Abstract: Legged robots have become a central focus in robotics research due to their superior ability to traverse rough terrains that hinder wheeled and tracked systems. One critical challenge in the design of quadruped robots is managing vertical ground contact forces during locomotion to prevent structural damage and improve efficiency. This study presents the design and analysis of a quadruped robot, focusing on the calculation of ground impact forces during movement across different surfaces. A five-bar linkage leg mechanism with two degrees of freedom per leg was modeled in MATLAB/Simulink 2023b. A physical prototype was fabricated using 3D printing with ABS material and controlled by Raspberry Pi and Arduino units. The ground contact forces were measured on hard and soft surfaces using force sensors and Wi-Fi-based data acquisition modules. The experimental results were in close agreement with the simulation data. On hard surfaces, the peak ground contact forces ranged between 12 and 14 N, indicating stable foot-ground interaction. Slight variations were observed on soft surfaces at the start of locomotion, attributed to terrain inconsistencies. The simulated forces were 6.61% higher than the experimental values on soft surfaces and 3.89% higher on hard surfaces, demonstrating high model accuracy within acceptable error margins. This study provides a comprehensive framework for improving quadruped robot design by integrating theoretical modeling and practical validation. The findings of this study contribute to the development of more stable and efficient robotic locomotion systems, enhancing performance across various ground types.

Keywords: Dynamic modeling; Ground contact force; Ground types interaction; SimMechanics^{TM}; Quadruped robot

1. Introduction

Legged robots have become a major focus in robotics research due to their superior mobility across real-world terrains, where wheeled and tracked systems often face limitations. Among these, quadruped robots have demonstrated significant potential in various applications, including search and rescue, exploration, and operations in harsh environments (Zhuang et al., 2024; Ding et al., 2024; Villaverde and Maneetham, 2024; Zhang, Li, et al., 2023; Rusdinar et al., 2021). Their primary advantage lies in their ability to maintain stable locomotion and effectively navigate obstacles on rough terrains, making them particularly valuable in high-mobility scenarios (Alwan et al., 2025; Alwan et al., 2024; Ha et al., 2024; Z. Wang et al., 2023; Qi et al., 2023; Sato et al., 2022). The mobility and balance control system in quadruped robots, particularly in adapting to vertical ground reaction forces during locomotion, presents significant challenges. Excessive contact forces between the robot's feet and the ground can cause structural deformation, reduced efficiency, and adverse effects on actuators and transmission systems (Hong et al., 2024; Kiefer et al., 2016). Additionally, energy loss due to impact forces during landing reduces the efficiency of the limited power supply of the robot (Zhang, Shen, et al., 2023; L. Wang et al., 2021).

https://doi.org/10.14716/ijtech.v17i1.7552
Received January 2025; Revised January 2025; Accepted April 2025

Recent research has focused on the development of dynamic walking and jumping mechanisms to enhance performance across varied terrains. Minimizing impact forces during landing is essential for maintaining the robot's operational integrity and longevity (Christie et al., 2023; Chignoli et al., 2022; Bakhy, 2014; Bakhy et al., 2013). (Zhang, Li, et al., 2023) introduced a novel landing planner concept that uses momentum feedback during flight phases to optimize landing positions, effectively reducing the impact of subsequent landing errors. Similarly, (Yang et al., 2021) proposed a symmetric-legged robot design equipped with high-density actuators to improve dynamic jumping capabilities and minimize impact forces. Other studies have explored passive and active control mechanisms to mitigate the impacts of landing. For example, (Christie et al., 2023) investigated the use of magnetorheological fluids for variable damping and stiffness control, achieving a 57.5% reduction in impact forces compared to rigid-legged structures. In addition, (Chignoli et al., 2022) introduced a hierarchical motion planning strategy for omnidirectional jumping, enhancing the ability of a quadruped robot to perform twisting jumps and rapid acceleration maneuvers. Moreover, Hooper et al., 2020 developed a compliant hopping mechanism powered by a direct current (DC) motor, using a flexure hinge-based structure to enable energy storage and controlled release during jumping.

To enhance landing and takeoff stability, a self-aligning cage with passive control mechanisms was incorporated. The design was further optimized through experimental testing, finite element analysis (FEA), and fabrication using 3D-printed PETG. Additionally, a hexapod robot simulator was developed using MATLAB SimMechanics™, integrating kinematic visualization with dynamic simulation to analyze the effects of gravity and mass on locomotion. A spring-damper model was implemented for foot-ground interactions to simulate realistic contact forces and rotational control dynamics. Research in ground contact force dynamics continues to focus on optimizing legged robot designs for improved stability and energy efficiency. (Menner and Berntorp, 2024) proposed an algorithm integrating contact detection and state estimation for legged robots, modeling their movement as a switched system with different modes based on foot-ground interactions. An interacting multiple-model Kalman filter is used to identify the active mode, enhancing the contact detection and state estimation accuracy. (Krishnamurthy et al., 2024) introduced a control architecture for legged-aerial multimodal robots, employing an optimization-free Explicit Reference Governor with external thruster forces from an attitude controller.

A conjugate momentum observer is used to estimate ground reaction forces, improving stability and control during locomotion. Cong et al., 2020 developed a contact force estimation technique for legged robots, enhancing stability control across various terrains by providing accurate ground reaction force estimation without relying on high-performance sensors. (Chopra et al., 2020) explored granular jamming feet, which passively modify foot stiffness upon ground contact, improving terrain adaptability and propulsion efficiency. Their study highlights the role of geometric and mechanical compliance in foot-ground interaction and impact absorption. (Xie et al., 2022) proposed a foot-ground interaction model based on stability contact optimization, incorporating a kinetic ground reaction force analysis using Hertz theory to enhance the realism and accuracy of robotic locomotion simulations. (Sombolestan and Nguyen, 2024) introduced an adaptive force-based control strategy for legged motion on uneven terrains, integrating adaptive control elements to improve dynamic movement and load-carrying capacity. The Unitree A1 robot demonstrated robust performance in high-speed trotting and bounding modes, even under uncertain terrain conditions. Their study developed a proprioception-based gait planner for predicting elevation changes and a two-degree-of-freedom tail mechanism to enhance stability and control during contactless motion. These mechanisms allow stabilization over elevation changes up to 1.5 times the leg length, even under tilted initial conditions.

This research aims to investigate and model the vertical ground reaction forces of quadruped robots in motion to study the surface contact behavior of the new leg design. A full model of a quadruped robot with legs and a five-bar mechanism was built using SimMechanics/MATLAB. This study focuses on developing and validating an accurate kinematic model for quadruped

robots, supported by experimental testing on various terrains, including stiff and soft surfaces. A comparative analysis was conducted between the experimental data and simulations in SimMechanics/MATLAB to evaluate the leg performance during trotting. This research aims to enhance locomotion efficiency, stability, and energy optimization, which are crucial for the next generation of quadruped robots. A key strength of this study lies in its integration of both simulation and experimental validation, which bridges the gap between theoretical modeling and real-world performance assessment. Unlike prior works that rely mainly on extrapolated simulations or limited testing, this study offers a comprehensive approach that improves the reliability of the results.

Additionally, the study examines foot-ground interaction across different surfaces (e.g., wood and ceramic) to assess terrain adaptability. The following sections detail the theoretical modeling, experimental setup, simulation results, and analysis of ground reaction forces, contributing to advancements in quadruped locomotion and impact force mitigation strategies.

2. Structure Design

Efficient locomotion in quadruped robots requires a stable mechanical design inspired by the joint configuration of quadruped mammals. The robot features a lightweight yet durable torso, which serves as the central structure for stabilizing the four legs. Each leg incorporates a five-bar linkage mechanism, providing three degrees of freedom (DOF) per leg, resulting in 12 DOF for the entire system. Motors are mounted on specialized brackets to facilitate movement, ensuring optimal power transmission to the joints. The upper torso control units manage command execution and motion data processing, enabling precise coordination and stability during locomotion.

2.1 Torso design

The torso of the quadruped robot is the primary structural component, integrating all four legs and providing mechanical stability. The design is optimized to meet functional and operational requirements, ensuring task execution efficiency and reliability. The design emphasizes strength, durability, and lightweight construction and prevents deformation or structural failure during locomotion, thereby enhancing maneuverability and energy efficiency while facilitating maintenance and repair. The robot's body was modeled using SolidWorks, with approximate dimensions of 450 mm $\times$ 250 mm $\times$ 150 mm. The design includes dedicated spaces for motor brackets and an external motor responsible for vertical actuation at the structure's four corners. The removable cover allows easy access to internal components, incorporating ventilation openings to regulate heat dissipation and protect sensitive electronics. The internal plate provides structural reinforcement and serves as a mounting base for motors, batteries, sensors, and control boards. It is securely fastened within the structure using screws to ensure stability. The front openings are designed to accommodate sensors, with protective covers shielding them from environmental factors.

Figure 1a illustrates the actuator holder, which was modeled using SolidWorks. The structure is hollow with openings at the top and bottom, with a wall thickness of 8 mm. To enhance durability and structural integrity, reinforced thickness is applied at mounting points and structural bridges. The servo motor bracket functions as a structural frame, securely mounting the motor to ensure stability and smooth operation. It is engineered to balance rigidity and lightweight construction, achieved through precise design and the selection of high-strength, low-weight materials. The outer dimensions of the bracket are approximately 59 mm $\times$ 52.3 mm $\times$ 33.56 mm, accommodating two motors (19.32 mm $\times$ 52.3 mm $\times$ 36.23 mm). The bracket features a protrusion on one side with a slot for securing it to the robot's frame using a pin, enhancing stability and allowing rotational movement. Bearings with inner and outer diameters of 8 and 16 mm, respectively, facilitate attachment, providing additional flexibility to the robot's leg. Additionally, the bracket includes openings for motor mounting, cable routing, and

weight reduction, contributing to improved efficiency and performance. To minimize overall weight without compromising structural integrity, unnecessary material sections are thinned or removed. The robot's body is fabricated using ABS material, ensuring deformation and breakage resistance. The body is divided into two segments (Figure 1b), connected using dovetail joints and screws based on the SolidWorks model. This modular design facilitates efficient 3D printing, assembly, and maintenance, enabling the independent modification or replacement of components without affecting the entire robot structure. Figure 2b illustrates the robot's assembled torso components.

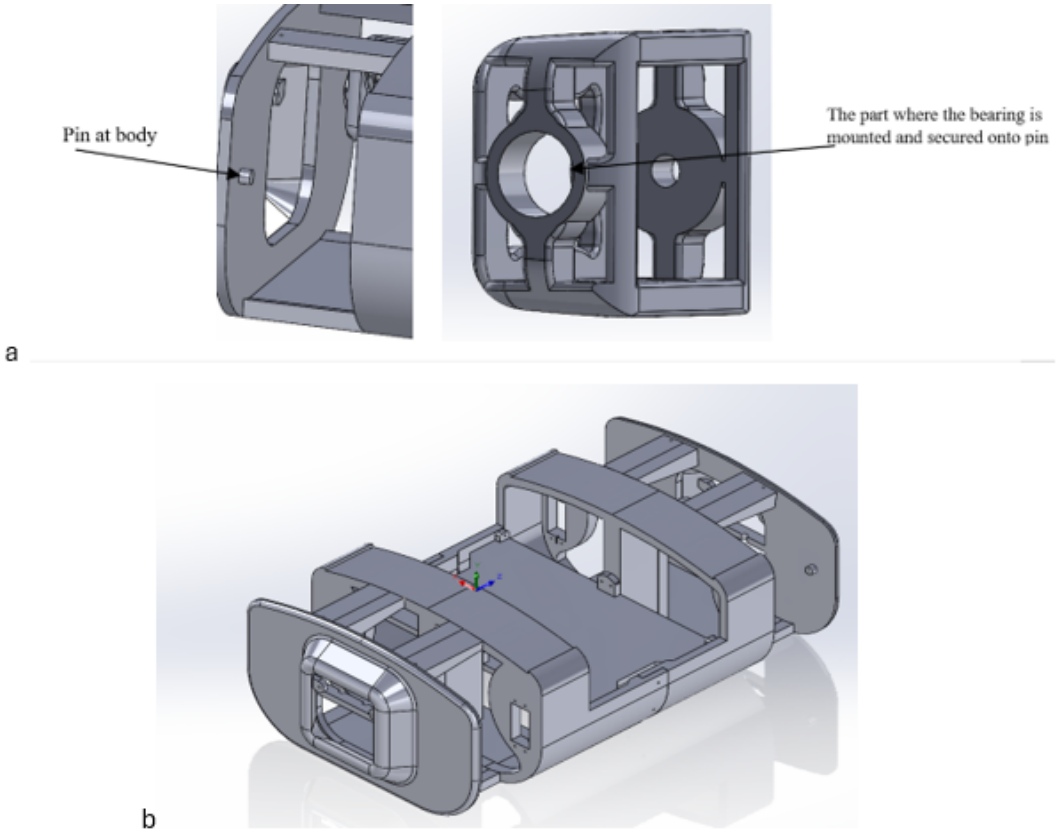

Figure 1 a. Explain the bracket fixed to the body using a pin in the body, b. The torso structure was designed using SolidWorks software

2.2 Design of the robotic leg

The robotic leg is designed based on a five-bar linkage mechanism, ensuring optimal kinematic performance through precise dimensional constraints and structural integrity. The linkage lengths were determined to satisfy kinematic modeling requirements, with the ground bar set to a minimum of 28 mm to provide adequate clearance for motor rotation. The first link measures 100 mm in length, with a width of 22.4 mm at the connection point, tapering to 12.25 mm, and a thickness of 10 mm. The design incorporates cavities for motor attachment and double bearings to connect with the second link, ensuring efficient torque transmission, smooth motion, and minimal friction. The second link, which is also 100 mm long, mirrors the first link in width and thickness. It features hex nut cavities at both ends, enabling secure fastening and eliminating unwanted movement, thereby enhancing stability and reducing surface friction. The third link, which measures 88 mm, interfaces with the motor and the second link. A curved extension, 92.24 mm long, is integrated to serve as the foot, improving strength, weight distribution, and load capacity. Curves on the surface of the foot enhance friction, promote even pressure distribution, and provide greater stability during locomotion.

This comprehensive design approach, modeled using SolidWorks, ensures that the robotic

leg performs efficiently across varying environmental conditions, contributing to enhanced balance, stability, and reduced mechanical stress. Upon completion of the design phase, the fabrication of components is carried out using 3D printing technology, with high-performance ABS materials selected to achieve a balance between lightweight construction and structural durability. These materials ensure the robot's structural integrity and support efficient operational performance. The printed components are assembled with motors and sensors in accordance with the SolidWorks-designed model, with meticulous attention to detail during assembly to ensure seamless integration between mechanical and electronic components. The motors are interfaced with control units using Arduino microcontrollers. Raspberry Pi, which manages the processing and motion control operations. The VNC program was used to access the Raspberry Pi, and a Python script was developed to control the robot's movements. The Raspberry Pi communicates with the Arduino by sending commands for forward, backward, left, and right movements of the robot through a serial port. Additionally, the Raspberry Pi retrieves GCF readings after converting the signal from analog to digital using the ADS1115 software. Batteries are installed within the frame to provide a reliable power source, while the wiring is strategically routed to ensure consistent performance and minimize electromagnetic interference and prevent power loss. The robot's front is equipped with distance sensors to enhance its spatial awareness and environmental mapping capabilities. A camera is installed to facilitate obstacle detection and prevent collisions during navigation. Force sensors are affixed at specific points on the robot's foot tips to enhance the dynamic response to movement and adapt to variations in surface characteristics. The force sensor (FSR 406) was utilized in this study due to its wide force measurement range (0.1–20 N) and high sensitivity to applied forces. A calibration curve was experimentally established to ensure a precise force-voltage relationship. The sensor's accuracy is estimated to be within ±5% to ±10%, depending on environmental conditions and signal processing techniques. A high-resolution analog-to-digital converter (ADS1115) was employed for data acquisition to mitigate measurement variations, and signal conditioning methods were applied during post-processing using MATLAB. All sensors, including the force sensors, are calibrated using the Raspberry Pi, enabling real-time data acquisition and analysis during operation. Figure 2 shows the quadratic robot structure.

Figure 2 Structure of the quadruped robot prototype illustrating the main mechanical and electronic components, including the body frame, front camera module, control unit (Raspberry Pi), battery pack, servo motors, five-bar linkage leg mechanism

After assembly, comprehensive field tests are conducted to evaluate the robot's performance under various operational conditions. The force sensor readings are recorded during the movement of the robot across different surfaces to analyze the effects of dynamic interaction with the

environment. This data provides insights into the capacity of the design model to withstand impacts by calculating the force and load-bearing capabilities, contributing to the optimization of the structural resilience of the robot.

3. Robotic Leg Kinematics

For analytical purposes, it consists of a five-bar mechanism, connected with the body by two revolute joints, both links L1 and L2 moved by two servo motors at points 1 and 4, and other links connected with other links by rotating joints (Figure 3).

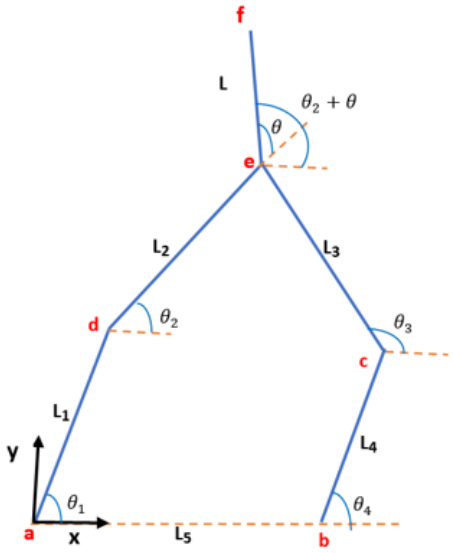

Figure 3 Configuration parameters of the 5-bar linkage robotic leg

The kinematics and dynamics of a robot leg are crucial for ensuring precise movement and control. This analysis enables the development of effective control algorithms and enhances the robot's ability to efficiently navigate and interact with its environment (Ahmadizadeh et al., 2023; Suomalainen et al., 2022; Chen et al., 2022; Deng et al., 2021; Zou et al., 2021). The forward kinematics equations for a 2-degree-of-freedom robotic leg have been calculated and are shown in (Ghose and Doss, 2023; Le Mesle et al., 2023; Antonov and Fomin, 2023; Alici, 2002) The equations represent the foot tip's position based on the angles of the two joints. The position of the foot tip is determined by combining the vectors from motor 1 to the foot link at point c.

$$\begin{aligned} x_c &= {L_1}^* \cos\theta_1 + {L_2}^* \cos\theta_2 \\ y_c &= {L_1}^* \sin\theta_1 + {L_2}^* \sin\theta_2 \end{aligned} \tag{1}$$

The foot tip position equations of adding up the vectors from motor 4 to the foot tip going through L3, L4, and L5 in the x and y directions are as follows:

$$\begin{aligned} x_c &= {L_3}^* \cos\theta_3 + {L_4}^* \cos\theta_4 + L_5 \\ y_c &= {L_3}^* \sin\theta_3 + {L_4}^* \sin\theta_4 \end{aligned} \tag{2}$$

The position of point f at the end of the foot with the ground:

$$x_f = {l_1}^* \cos\theta_1 + {l_2}^* \cos\theta_2 + {l}^* \cos(\theta + 2\arctan(\theta_2)) \tag{3}$$

$$y_f = {l_1}^* \sin\theta_1 + {l_2}^* \sin\theta_2 + {l}^* \sin(\theta + 2\arctan(\theta_2)) \tag{4}$$

The Jacobi matrix of tiptoe J_h is obtained as follows (Sato, Arita and Ming, 2022):

$$J_h = \begin{bmatrix} (L_1 + L_3)C_h + L_2C_{ck} & -L_2C_{hk} \\ (L_1 + L_3)S_h + L_2S_{hk} & -L_2S_{hk} \end{bmatrix} \tag{5}$$

The proximity torque to each joint, τ_s, is calculated as follows:

$$\tau_s = J_h(\theta)^T F_s \tag{6}$$

4. Simmechanics Modeling of the Robot Leg

The robot leg model was simulated using SimMechanics^{TM}, which offers significant advantages due to its user-friendly interface, facilitating the direct integration of model features from SolidWorks designs. Additionally, variables can be easily imported and exported to and from MATLAB, making SimMechanics^{TM} a comprehensive tool that ensures seamless communication with other Simulink tools, thereby simplifying the modeling process (Le and Vo, 2024; Saravana Mohan et al., 2024; Ansari and Shahnawaz, 2023; Nugroho et al., 2023). This study presents a model for simulating foot-ground interaction in a quadruped robot using the SimMechanics^{TM} environment and develops a tool for optimizing the performance of legged robots. In general, the quadruped robot is modeled based on the following assumptions:

- Negligible internal friction: Internal friction effects are considered minimal, allowing for emphasis on external forces.
- Constant speed: The robot maintains a consistent locomotion speed during the experiments.

These assumptions streamline the model while ensuring practical validation within the constraints of the study. In this model, four blocks represent the different links of the robot leg, while the blocks on the right side represent the initial angles of each joint during the simulation, as illustrated in Figure 4. The subsystem connects the right main body block with the left foot block. At the end of the robot's foot, a spherical block with a radius of r=2 cm is incorporated to simulate ground interaction.

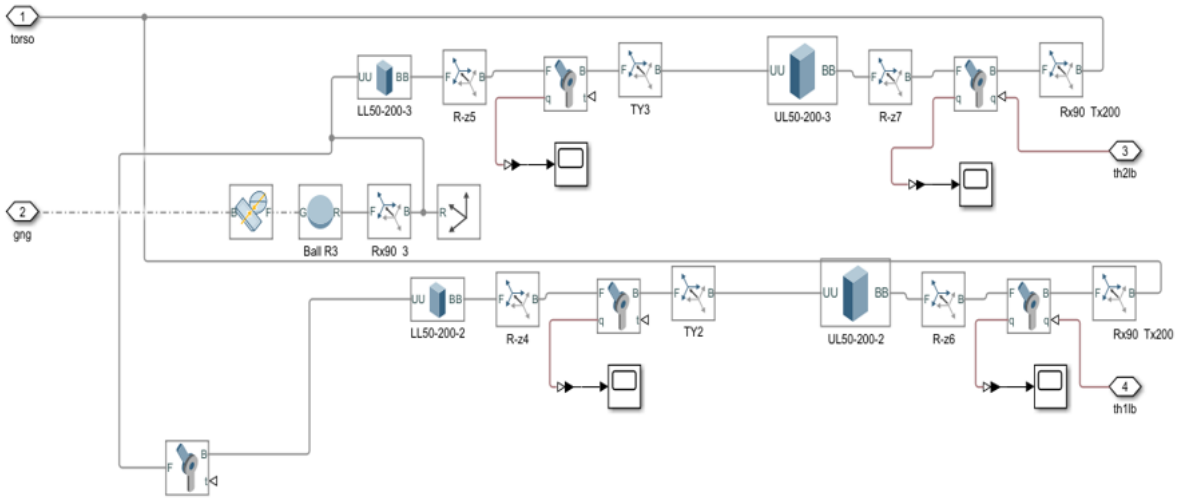

Figure 4 Model of the robot's leg

The ground interaction model constitutes a critical component of the robot, as an equal and opposite force is exerted on the foot once the robot's foot makes contact with the ground, in accordance with Newton's third law. This interaction drives the body's movement across the given surface. A contact point is represented at the end of the robot leg to simplify the model, where a three-dimensional force is applied to the ground, and an equal magnitude force

in the opposite direction acts on the robot's foot. The resulting force is decomposed into two components: one along the x-axis and the other along the y-axis. Ground subsystems were implemented to simulate the quadruped robot realistically.

Equations 7 and 8 are used to estimate the applied forces, which is represented as (Silva et al., 2005). It is activated only when the foot is in contact with the ground:

$$F_x = -K_x(x - x_0) - B_x\dot{x} \tag{7}$$

$$F_y = -K_y y - B_y(-y)^m\dot{y} \tag{8}$$

Where F_x represents the tangential (friction) force along the x-axis, K_x is the sp'sng's elastic constant, x and xo are the current and reference positions, B_x is the damping coefficient, and $x^{\cdot}$ is the velocity along the x-axis. Similarly, F_y denotes the normal force along the y-axis, K_y is the sp'sng's elastic constant, y is the current position, B_y is the damping coefficient, m is a factor influenced by surface conditions, and $y^{\cdot}$ is the velocity along the y-axis. The interaction between the robot's foot and the ground is modeled using a spring-damper system with a spring stiffness of 5000 N/m and a damping coefficient of 10 Ns/m. This approach accurately captures dynamic impact forces, enhancing the simulation precision for analyzing the robot's stability and control. The frictional force is based on a smooth spring-damper system, while the normal force is represented by a nonlinear spring-damper equation, selected for its superior performance in tests. This study considers two primary components of the contact interaction: the normal force that keeps the robot elevated above the ground and the tangential force that propels the robot forward.

5. Results and Discussion

The dynamic modeling of the quadruped robot was conducted using MATLAB/Simulink 2023b, incorporating the body and 5-bar leg mechanism of the robot. The simulation was performed during the robot's walking phase to evaluate its kinematic and dynamic performance. Figure 5 illustrates the angular displacement at different joints over time, providing insight into joint behavior during locomotion. Figure 5a highlights the angular position of joint (a), demonstrating a consistent oscillatory pattern over a 50-s interval. This oscillation indicates a stable periodic motion, which is essential for maintaining the gait of the robot. Figure 5d presents the angular movement of joint (e), showing similar periodic characteristics but with reduced amplitude, suggesting a compensatory movement that enhances overall balance. Further analysis in Figure 5b focuses on joint (b), revealing a phase-shifted oscillation, while Figure 5c indicates the position of joint (d) with greater variation in amplitude, highlighting its critical role in foot placement during contact and flight phases.

During the simulation, the peak torque at joint (a) (first actuator) was measured at 8 $\mathrm{N \cdot cm}$, as shown in Figure 6a, while joint (e) (second actuator) exhibited a higher peak torque of approximately 12 $\mathrm{N \cdot cm}$, as shown in Figure 6b. These results highlight the varying load distribution across different joints, with joint (e) experiencing greater mechanical stress during the locomotion cycle of the robot.

A flat surface was used in the simulation, and a smooth spring-damper system was applied during ground contact. This approach aligns with the findings of Chopra et al., 2020, who showed that granular jamming feet enhanced robot stability on deformable surfaces. The ground contact force (GCF) for the legs of the quadruped robot during trotting motion on hard and soft surfaces was analyzed using force sensors and simulations. The results demonstrated a high degree of agreement between the experimental data and the simulations.

Force curves exhibiting a recurring pattern of peaks and valleys, reflecting the gait's dynamic stability. On hard surfaces, as shown in Figure 7, the GCF values ranged between 12 and 14 N, with sharp peaks indicating direct foot-ground impacts. This aligns with the findings of Cong et al., 2020, who reported similar ground contact dynamics for legged robots on hard surfaces. Christie et al., 2023 also highlighted the effectiveness of magnetorheological dampers

in mitigating impact forces, aligning with the observed stability of robot movement on hard surfaces.

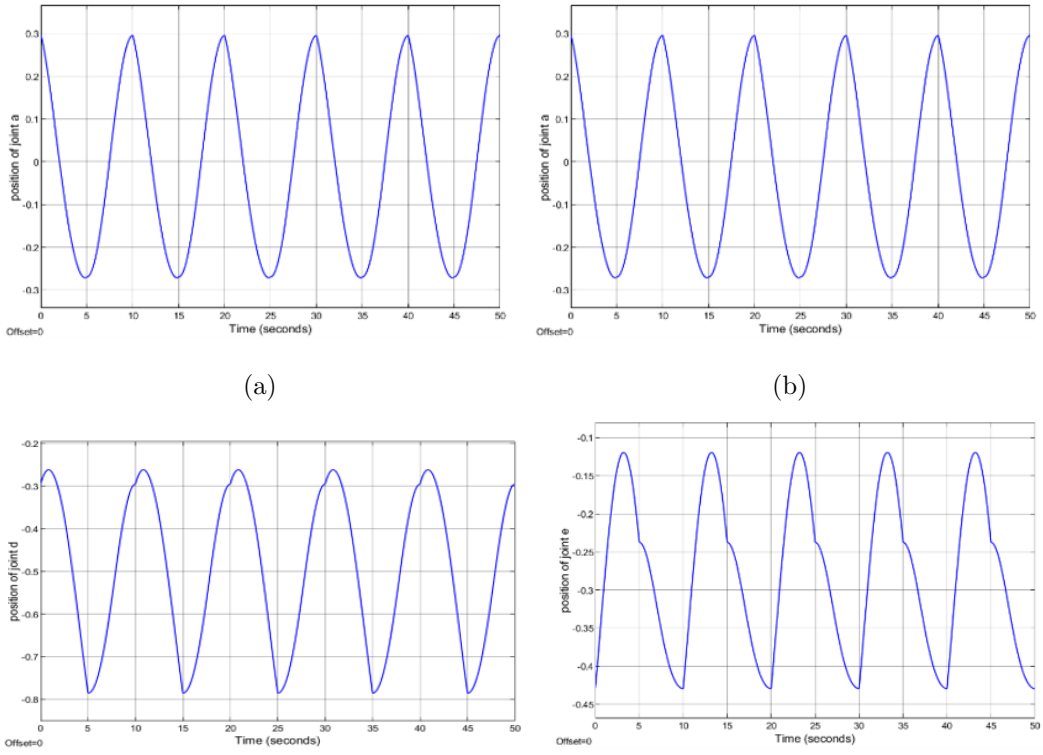

Figure 5 Position of all joints in the robotic leg (a) Position of joint a, (b) Position of joint b, (c) Position of joint d, (d) Position of the joint e

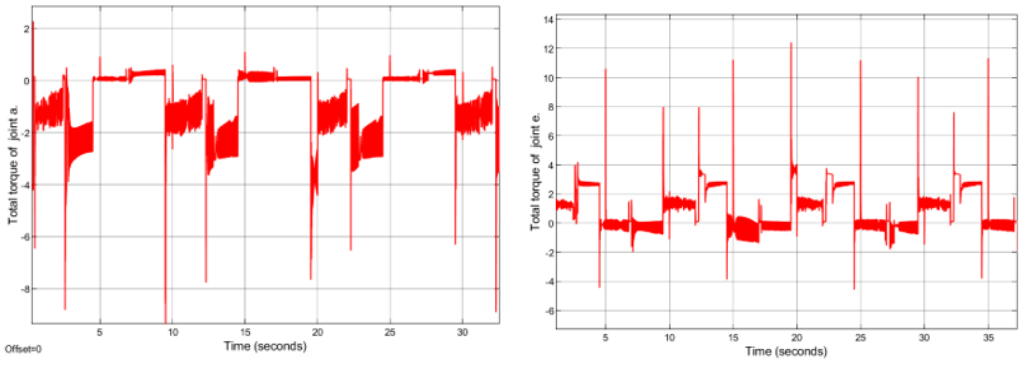

Figure 6 Torque of actuators at the robotic leg (a) Position of the first actuator (b) Position of the second actuator

Figure 8 explains the results at soft surfaces. It showed stable peaks with slight variations at the beginning of the motion, attributed to minor terrain interaction inconsistencies. This is consistent with the work of Hong et al., 2024, who confirmed that soft surfaces provide reliable contact but lead to variations in peak force due to the ground types' flexible nature. Ding et al., 2024 emphasized the role of elastic components in reducing impact forces during jumping, which is consistent with the results observed on soft surfaces, which provided more sustained but less stable contact than hard surfaces. The results affirm the significance of force distribution, reinforcing the findings of Qi et al., 2023, who employed active compliance control to manage vertical jumps and mitigate impact forces.

The errors observed in the results are directly related to the assumptions of the modeling.

The Coulomb friction model used for ground contact assumes a rigid interface, ignoring micro-deformations that may influence the force distribution. Additionally, the assumption of rigid robot legs disregards minor flexibilities in the ABS material and joint clearances, potentially affecting force measurements. Sensor limitations, including measurement noise and resolution constraints, contribute to variations in recorded values, particularly in high-frequency impact events. Finally, environmental inconsistencies, such as surface texture variations and sensor placement errors, introduce additional discrepancies between the experimental and simulated data. These factors collectively impact the model's accuracy, highlighting the need for refined ground interaction modeling and consideration of structural compliance in future studies.

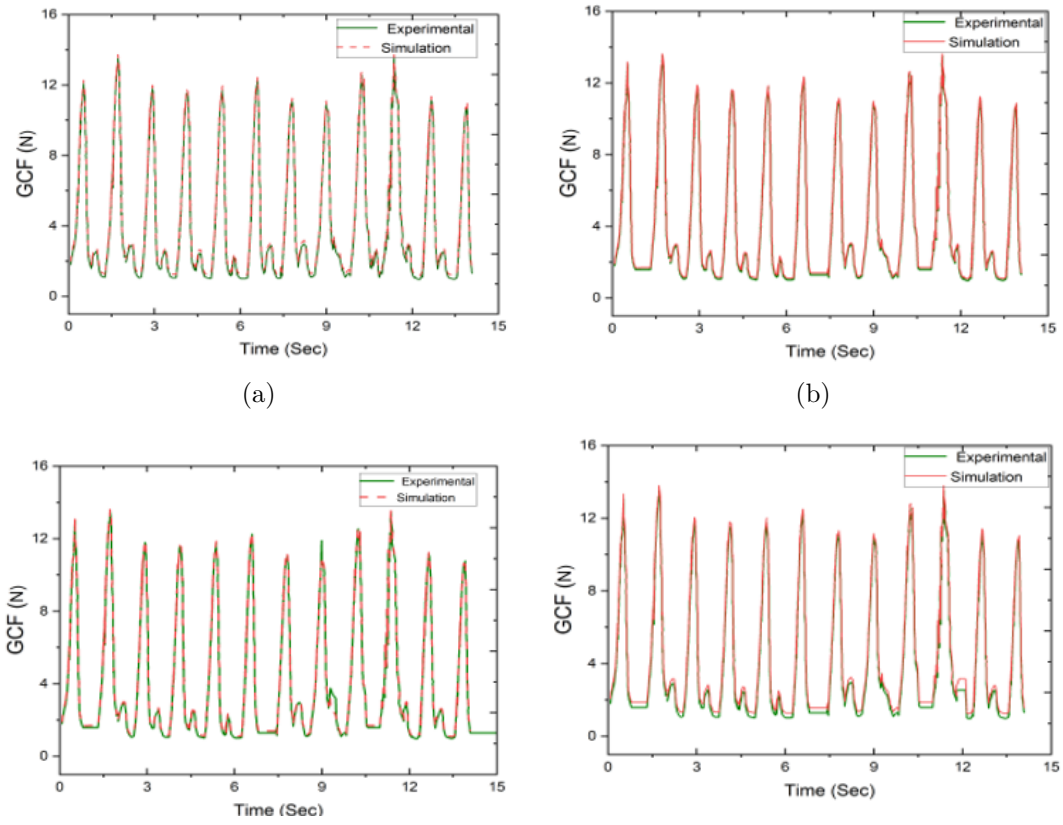

Figure 7 Ground contact force analysis of the quadruped robot on a stiff surface during trotting motion (a) the left backside leg, (b) Right Backside Leg, (c) Right front side Leg, (d) Left front side Leg

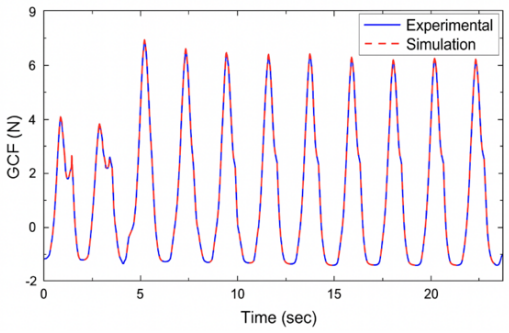

Figure 8 Ground contact force analysis of the quadruped robot on a soft surface during trotting motion

This study confirms the effectiveness of simulation models in representing the locomotion of quadruped robots across various terrains. The results highlight that hard surfaces provide

higher GCF values and greater stability than soft surfaces, underscoring the need to consider these differences in future robot designs to ensure more stable and efficient movement.

6. Conclusions

This study demonstrates the effectiveness of dynamic modeling and simulation in evaluating the kinematic and dynamic performance of a quadruped robot using MATLAB/Simulink 2023b. The analysis of ground contact forces across different surfaces highlights the significant impact of terrain properties on robotic stability. GCF values ranged between 12 and 14 N on stiff surfaces, with sharp peaks indicating stable and direct foot-ground contact. On soft surfaces, while the peaks remained stable, minor variations were observed at the start of motion due to terrain inconsistencies. The experimental validation confirmed that the quadruped robot, controlled via Raspberry Pi and Arduino, reliably measured the ground contact forces. The results indicate that the simulated GCF values exceeded the experimental values by approximately 6.61% and 3.89% on soft and hard surfaces, respectively. These discrepancies fall within acceptable scientific limits, reinforcing the simulation model's accuracy and demonstrating its potential for optimizing robot performance across diverse environments.

Acknowledgements

The authors would like to express their deepest gratitude to the University of Technology/Department of Mechanical Engineering for their invaluable support and assistance throughout this research.

Author Contributions

Zaineb W. Matteb; Methodology, Derivation of Robot Kinematic and Dynamic Models and Formal Analysis, Bakhy S. H. Review and supervision, Nabil H. H.; simulation of results, software, and project administration. All authors have read and approved the published version of the manuscript.

Conflict of Interest

The authors have no conflicts of interest to declare. They confirmed that no personal circumstances or financial interests could have inappropriately influenced the representation or interpretation of the research results.

References

Ahmadizadeh, M., Shafei, A. M., & Fooladi, M. (2023). Dynamic modeling of closed-chain robotic manipulators in the presence of frictional dynamic forces: A planar case. *Mechanics Based Design of Structures and Machines*, *51*(8), 4347–4367. https://doi.org/https://doi.org/10.1080/15397734.2021.1966304

Alici, G. (2002). An inverse position analysis of five-bar planar parallel manipulators. *Robotica*, *20*, 195–201. https://doi.org/https://doi.org/10.1017/S0263574701003666

Alwan, H. M., Nikolaevic, A. V., Hasan, S. F., & Vladmerovna, O. K. (2024). Kinematic and dynamic modeling based on trajectory tracking control of mobile robot with mecanum wheels. *International Journal of Technology*, *15*(5), e5901. https://doi.org/https://doi.org/10.14716/ijtech.v15i5.6908

Alwan, H. M., Nikolavich, A. V., Shbani, A., & Kochneva, O. V. (2025). Motion control and obstacle avoidance of mobile robot with mecanum wheels. *International Journal of Technology*, *16*(1). https://doi.org/https://doi.org/10.14716/ijtech.v16i1.7254

Ansari, B., & Shahnawaz, S. (2023). Modeling and control of a snake robot using simmechanics. *Sukkur IBA Journal of Emerging Technologies*, *6*(2), 1–10. https://doi.org/https://doi.org/10.30537/sjet.v6i2.1378

Antonov, A., & Fomin, A. (2023). Mechanism design and inverse kinematics of a 5-dof medical assistive manipulator. *International Workshop on Medical and Service Robots*, 334–342. https://doi.org/https://doi.org/10.1007/978-3-031-32446-8_36

Bakhy, S. H. (2014). Modeling of contact pressure distribution and friction limit surfaces for soft fingers in robotic grasping. *Robotica*, *32*(7), 1005–1015. https://doi.org/https://doi.org/10.1016/j.rob.2014.09.010

Bakhy, S. H., Hassan, S. S., Nacy, S. M., Dermitzakis, K., & Arieta, A. H. (2013). Contact mechanics for soft robotic fingers: Modeling and experimentation. *Robotica*, *31*(4), 599–609. https://doi.org/https://doi.org/10.1017/S0263574713001215

Chen, Y., Sun, Q., Guo, Q., & Gong, Y. (2022). Dynamic modeling and experimental validation of a water hydraulic soft manipulator based on an improved newton–euler iterative method. *Micromachines*, *13*(1), 130. https://doi.org/https://doi.org/10.3390/mi13010130

Chignoli, M., Morozov, S., & Kim, S. (2022). Rapid and reliable quadruped motion planning with omnidirectional jumping. *Proceedings of the IEEE International Conference on Robotics and Automation*, 6621–6627. https://doi.org/https://doi.org/10.48550/arXiv.2111.13648

Chopra, S., Tolley, M. T., & Gravish, N. (2020). Granular jamming feet enable improved foot–ground interactions for robot mobility on deformable ground. *IEEE Robotics and Automation Letters*, *5*(3), 3975–3981. https://doi.org/https://doi.org/10.1109/LRA.2020.2982361

Christie, M. D., Sun, S., Deng, L., Du, H., Zhang, S., & Li, W. (2023). Shock absorption for legged locomotion through magnetorheological leg-stiffness control. *Machines*, *11*(2), 236. https://doi.org/https://doi.org/10.3390/machines11020236

Cong, Z., Wu, C., Lang, L., Wei, Q., & Ma, H. (2020). Contact force estimation method of legged robot and its application in impedance control. *IEEE Access*, *8*, 161175–161187. https://doi.org/https://doi.org/10.1109/ACCESS.2020.3021080

Deng, J., Shang, W., Zhang, B., Zhen, S., & Cong, S. (2021). Dynamic model identification of collaborative robots using a three-loop iterative method. *Proceedings of the IEEE International Conference on Advanced Robotics and Mechatronics*, 937–942. https://doi.org/https://doi.org/10.1109/ICARM52023.2021.9536165

Ding, J., Atanassov, V., Panichi, E., Kober, J., & Santina, C. D. (2024). Robust quadrupedal jumping with impact-aware landing: Exploiting parallel elasticity. *IEEE Transactions on Robotics*. https://doi.org/https://doi.org/10.1109/TRO.2024.3411988

Ghose, D., & Doss, A. S. A. (2023). Optimal kinematic design of a robotic lizard using four-bar and five-bar mechanisms [arXiv preprint arXiv:2308.08151]. https://doi.org/https://doi.org/10.48550/arXiv.2308.08151

Ha, V. T., Thuong, T. T., & Thanh, N. T. (2024). Design of adjustable slider controller in combination with a* algorithm in motion control for mobile robot. *International Journal of Technology*, *15*(5), 1487–1501. https://doi.org/https://doi.org/10.14716/ijtech.v15i5.6527

Hong, C., Tang, D., Quan, Q., Cao, Z., & Deng, Z. (2024). Energy-recoverable landing strategy for small-scale jumping robots. *Robotics and Autonomous Systems*, *176*, 104696. https://doi.org/https://doi.org/10.1016/j.robot.2024.104696

Hooper, J., Garcia, M., Pena, P., & Tekes, A. (2020). Design of a compliant jumping robot with passive stabilizer. *Proceedings of the ASME International Mechanical Engineering Congress and Exposition*, V07BT07A019. https://doi.org/https://doi.org/10.1115/IMECE2020-23171

Kiefer, J., Ward, M., & Costello, M. (2016). Rotorcraft hard landing mitigation using robotic landing gear. *Journal of Dynamic Systems, Measurement, and Control*, *138*(3), 031003. https://doi.org/https://doi.org/10.1115/1.4032286

Krishnamurthy, K. V., Wang, C., P, S., Sihite, E., R, A., & G, M. (2024). Optimization-free control and ground force estimation with momentum observer for a multimodal legged aerial robot [arXiv preprint arXiv:2411.11216]. https://doi.org/https://doi.org/10.48550/arXiv.2411.11216

Le, H. N., & Vo, N. T. (2024). Modeling and analysis of an ruu delta robot using solidworks and simmechanics. *International Journal of Dynamics and Control*, 1–13. https://doi.org/https://doi.org/10.1007/s40435-023-01377-1

Le Mesle, V., Bégoc, V., & Briot, S. (2023). Modeling and design of a five degrees-of-freedom delta-like robot for fast pick-and-place applications. *Journal of Mechanical Design*, *145*(12), 235. https://doi.org/https://doi.org/10.1115/1.4063359

Menner, M., & Berntorp, K. (2024). Simultaneous state estimation and contact detection for legged robots by multiple-model kalman filtering [arXiv preprint arXiv:2404.03444]. https://doi.org/https://doi.org/10.23919/ECC64448.2024.10590751

Nugroho, H. A., Cahyadi, A. I., & Ardiyanto, I. (2023). Trajectory tracking control of quadrotor using lq-servo control with simmechanics. *10*(4), 2412–2422. https://doi.org/https://doi.org/10.5109/7160931

Qi, H., Chen, X., Yu, Z., Huang, G., Liu, Y., & Meng, L. (2023). Vertical jump of a humanoid robot with cop-guided angular momentum control and impact absorption. *IEEE Transactions on Robotics*, *39*, 3154–3166. https://doi.org/https://doi.org/10.1109/TRO.2023.3271136

Rusdinar, A. I., Purnama, A., Fuadi, A. Z., Adiluhung, H., Wicaksono, M., & Ningrum, R. A. (2021). Automated ultraviolet c light mobile robot for room sterilization and disinfection. *International Journal of Technology*, *12*(4), 854–864. https://doi.org/https://doi.org/10.14716/ijtech.v12i4.4817

Saravana Mohan, M., Kumar, P. S. R., & Mashinini, P. M. (2024). Sustainable development of redundant articulated robot components using simscape multibody. In *Sustainable machining and green manufacturing* (pp. 193–219). https://doi.org/https://doi.org/10.1002/9781394197866.ch10

Sato, R., Arita, H., & Ming, A. (2022). Pre-landing control for a legged robot based on tiptoe proximity sensor feedback. *IEEE Access*, *10*, 21619–21630. https://doi.org/https://doi.org/10.1109/ACCESS.2022.3153127

Silva, M. F., Machado, J. A. T., & Lopes, A. M. (2005). Modeling and simulation of artificial locomotion systems. *Robotica*, *23*(5), 595–606. https://doi.org/https://doi.org/10.1017/S0263574704001195

Sombolestan, M., & Nguyen, Q. (2024). Adaptive force-based control of dynamic legged locomotion over uneven terrain. *IEEE Transactions on Robotics*, *40*(9), 233–233. https://doi.org/https://doi.org/10.1109/TRO.2024.3381554

Suomalainen, M., Karayiannidis, Y., & Kyrki, V. (2022). A survey of robot manipulation in contact. *Robotics and Autonomous Systems*, *156*, 104224. https://doi.org/https://doi.org/10.1016/j.robot.2022.104224

Villaverde, L., & Maneetham, D. (2024). Kinematic and parametric modeling of 6dof industrial welding robot design and implementation. *International Journal of Technology*, *15*(4). https://doi.org/https://doi.org/10.14716/ijtech.v15i4.6559

Wang, L., Meng, F., Kang, R., Chen, X., Yu, Z., Ming, A., & Huang, Q. (2021). Design and implementation of symmetric legged robot for highly dynamic jumping and impact mitigation. *Sensors*, *21*(20), 6885. https://doi.org/https://doi.org/10.3390/s21206885

Wang, Z., Chen, C., Chen, J., & Zheng, G. (2023). 3d soft-landing dynamic theoretical model of legged lander: Modeling and analysis. *Aerospace*, *10*(9), 811. https://doi.org/https://doi.org/10.3390/aerospace10090811

Xie, Z., Li, L., & Luo, X. (2022). A foot-ground interaction model based on contact stability optimization for legged robot. *Journal of Mechanical Science and Technology*, *36*(2), 921–932. https://doi.org/https://doi.org/10.1007/s12206-022-0139-1

Yang, J., Sun, H., An, H., & Wang, C. (2021). Impact mitigation for dynamic legged robots with steel wire transmission using nonlinear active compliance control. *Proceedings of the IEEE International Conference on Robotics and Automation*, 2525–2531. https://doi.org/https://doi.org/10.48550/arXiv.2108.01481

Zhang, J., Li, M., Cao, J., Dou, Y., & Xiaoyan, X. (2023). Research on bionic jumping and soft landing of single leg system in quadruped robot. *Journal of Bionic Engineering*, *20*(5), 2088–2107. https://doi.org/https://doi.org/10.1007/s42235-023-00360-y

Zhang, J., Shen, J., Liu, T., & Hong, D. (2023). Design of a jumping control framework with heuristic landing for bipedal robots. *Proceedings of the IEEE/RSJ International Conference on Intelligent Robots and Systems*, 8502–8509. https://doi.org/https://doi.org/10.48550/arXiv.2304.00536

Zhuang, H., Wang, J., Wang, N., & Li, W. (2024). A review of foot–terrain interaction mechanics for heavy-duty legged robots. *Applied Sciences*, *14*(15), 6541. https://doi.org/https://doi.org/10.3390/app14156541

Zou, Q., Zhang, D., Zhang, S., & Luo, X. (2021). Kinematic and dynamic analysis of a 3-dof parallel mechanism. *International Journal of Mechanics and Materials in Design*, *17*(3), 587–599. https://doi.org/https://doi.org/10.1007/s10999-021-09548-8